Published in final edited form as:
Exp Neurol. 2014 November ; 0: 553–562. doi:10.1016/j.expneurol.2014.08.001.

The first knockin mouse model of episodic ataxia type 2

Samuel J. Rose[1], **Lisa H. Kriener**[1], **Ann K. Heinzer**[2], **Xueliang Fan**[1], **Robert S. Raike**[1], **Arn M.J.M. van den Maagdenberg**[3], and **Ellen J. Hess**[1,4]

[1]Department of Pharmacology, Emory University School of Medicine, Atlanta, GA 30322, USA [2]Department of Neuroscience, Johns Hopkins University School of Medicine, Baltimore, MD 21287, USA [3]Departments of Human Genetics and Neurology, Leiden University Medical Centre, 2300 RC Leiden, The Netherlands [4]Department of Neurology, Emory University School of Medicine, Atlanta, GA 30322, USA

Abstract

Episodic ataxia type 2 (EA2) is an autosomal dominant disorder associated with attacks of ataxia that are typically precipitated by stress, ethanol, caffeine or exercise. EA2 is caused by loss-of-function mutations in the *CACNA1A* gene, which encodes the α_{1A} subunit of the $Ca_V2.1$ voltage-gated Ca^{2+} channel. To better understand the pathomechanisms of this disorder *in vivo*, we created the first genetic animal model of EA2 by engineering a mouse line carrying the EA2-causing c.4486T>G (p.F1406C) missense mutation in the orthologous mouse *Cacna1a* gene. Mice homozygous for the mutated allele exhibit a ~70% reduction in $Ca_V2.1$ current density in Purkinje cells, though surprisingly do not exhibit an overt motor phenotype. Mice hemizygous for the knockin allele (EA2/− mice) did exhibit motor dysfunction measurable by rotarod and pole test. Studies using Cre-flox conditional genetics explored the role of cerebellar Purkinje cells or cerebellar granule cells in the poor motor performance of EA2/− mice and demonstrate that manipulation of either cell type alone did not cause poor motor performance. Thus, it is possible that subtle dysfunction arising from multiple cell types is necessary for the expression of certain ataxia syndromes.

Keywords

ataxia; episodic ataxia type 2; EA2; channelopathy; CACNA1A; voltage-gated calcium channel; Purkinje cell; cerebellar granule cell; Cre; knockin

Corresponding author: Ellen J. Hess, Departments of Pharmacology and Neurology, Emory University School of Medicine, 101 Woodruff Circle, WMB 6303, Atlanta, GA 30322. + 1 404 727 4911. ellen.hess@emory.edu.

Introduction

Episodic ataxia type 2 (EA2) is an autosomal dominant disorder characterized by a relatively normal neurological baseline and attacks of ataxia that are typically precipitated by stress, ethanol (EtOH), caffeine or exercise (Jen et al., 2007, Baloh, 2012, Rajakulendran et al., 2012). EA2 is caused by specific mutations in the *CACNA1A* gene, which encodes the α_{1A} subunit of the $Ca_V2.1$ (P/Q-type) voltage-gated Ca^{2+} channel. Dozens of EA2 mutations have been identified in the *CACNA1A* gene including nonsense, deletion or splice site mutations that abrogate $Ca_V2.1$ channel function and missense mutations encoding hypoconductive $Ca_V2.1$ channels (Tomlinson et al., 2009, Pietrobon, 2010).

Although it has been well established that EA2 mutations most often lead to a loss of channel function and reduction in whole-cell $Ca_V2.1$ Ca^{2+} current, the pathomechanisms are still debated. It has been suggested that EA2 mutant channels suppress normal $Ca_V2.1$ channel function through a dominant-negative mechanism, comparable to a total knockout of channel function (Jeng et al., 2006, Raike et al., 2007, Jeng et al., 2008, Mezghrani et al., 2008). However, other studies suggest that EA2 is caused by mere haploinsufficiency of $Ca_V2.1$ currents (Wappl et al., 2002, Imbrici et al., 2004, Imbrici et al., 2005). Indeed even where mutant channel properties are well characterized by multiple laboratories *in vitro*, such as the c.4486T>G (p.F1406C) missense mutation (Jen et al., 2001, Jeng et al., 2006, Jeng et al., 2008), the disease-causing mechanism is unresolved.

Consistent with the association between ataxic disorders and cerebellar dysfunction, $Ca_V2.1$ channels are highly expressed in cerebellar Purkinje cells (PCs) and cerebellar granule cells (GCs) and both cell types are sensitive to changes in $Ca_V2.1$ conductance (Regan, 1991, Randall and Tsien, 1995). Furthermore, PCs are the sole output neurons of the cerebellar cortex and PC-specific lesions induce ataxia in humans and animal models (Holmes, 1917, Diener and Dichgans, 1992, Feddersen et al., 1992). Indeed, selective elimination of $Ca_V2.1$ channels from PCs causes a severe and chronic motor syndrome in mice that includes ataxia (Mark et al., 2011, Todorov et al., 2012). In other spontaneous mouse mutants with point mutations within *Cacna1a* that lead to moderately hypoconductive $Ca_V2.1$ channels, the motor dysfunction is somewhat less severe with both chronic and episodic components (Wakamori et al., 1998, Kodama et al., 2006, Shirley et al., 2008). However, in the heterozygous state, where one wild-type *Cacna1a* allele remains, mutant mice have normal motor function. Yet, heterozygsity in humans with EA2 is sufficient to cause attacks of ataxia. Therefore, to specifically address questions of EA2 pathomechanisms *in vivo*, we generated the first EA2 knockin mice bearing the human pathogenic p.F1406C missense mutation, which results in a severely hypoconductive channel with only 10–20% residual current (Jen et al., 2001).

Materials and Methods

EA2 knockin mice

Recombineering methods and vectors from NCI-Frederick (http://ncifrederick.cancer.gov/research/brb/reagents/recombineeringReagent.aspx) were used to prepare the targeting construct. A C57BL/6 BAC clone was identified from the RPCI23 BAC library. RP23–

275N4, which encompassed exons 2–46 of mouse *Cacna1a*, was confirmed by endonuclease restriction digest and diagnostic PCRs (not shown). The EA2-causing F1406C mutation was introduced into exon 26 by site-directed mutagenesis. The targeting vector also contained, a PGK-driven neomycin (neo^r) cassette flanked by two loxP sites downstream of exon 26. C57BL/6-derived embryonic stem cells were electroporated with the targeting construct and clones were screened for homologous recombination by Southern blot. The presence of the c.4486T>G mutation was confirmed by polymerase chain reaction (PCR) amplification of exon 26 with forward and reverse primers 5'-GGAAACCAGAAGCTGAACCA-3' and 5'-CCCTGAATTCCTCCATTTC-3', and endonuclease digestion of the PCR product with the enzyme *BstAPI*, or sequencing of the PCR product. Targeted ES cells were injected into blastocysts to produce chimeric mice. Mice with germline transmission were identified and long PCR from genomic DNA of F1 progeny was used as an additional screen to confirm homologous recombination of the targeting construct in the mice (Fig. 1A). The 5' insertion site was verified by two reactions (P1-P2 and P1-P3) that used a common forward primer specific to the genomic DNA upstream of and outside of the 5' end of the construct, P1, 5'-TCCTGCCCAGTACAGAGATTGA-3', and a reverse primer upstream of the neo^r, P2, 5'-GAATTCAAGCTTCACTGGGAGACTAG-3', and one specific to the neo^r, P3, 5'-AGGCCAGAGGCCACTTGTGTAG-3'. The 3' insertion site was confirmed by two reactions (P4-P6 and P5-P6) that used a common reverse primer specific to the genomic DNA downstream and outside of the 3' end of the construct, P6, 5'-CCCTAAACTTTTTCAGCCCAAAGG-3', and one forward primer specific to the neo^r, P4, 5'-GACGAGTTCTTCTGAGGGGATCAA-3', and one downstream of the neo^r, P5, 5'-GGAGGATCACCCTGAGTTTTGAGA-3'. The PCR product of a short amplicon (325 bp) encompassing the c.4486T>G mutation was also sequenced, verifying that mice testing positive for the long PCR assay also carried the point mutation. Mice carrying the unresolved knockin allele were crossed with the Cre-deleter strain C57BL/6-Tg(Zp3-Cre)93Knw/J (The Jackson Laboratory, Bar Harbor, ME) to remove the neomycin cassette. Progeny carrying the resolved allele were crossed with C57BL/6J mice to segregate the Cre allele. These EA2 knockin mice, which were coisogenic with C57BL/6J, were bred and maintained on a C57BL/6J background. For subsequent genotyping of EA2 knockin mice, PCR amplicons were sequenced as above or quantitative PCR was used (not shown).

Other mouse lines

Mice carrying a knockout *Cacna1a* allele (+/−) on a mixed C3H–C57BL/6J background were kindly provided by Dr. David Yue (Johns Hopkins University). Mice carrying a floxed *Cacna1a* allele (flox/+) on a C57BL/6J background were previously described (Todorov et al., 2006). Mice carrying the Tg(Pcp2-Cre)2Mpin/J (L7-Cre/-) transgene on a C57BL/6J background were obtained from The Jackson Laboratory and were used to drive recombination specifically in PCs. Mice carrying the Math1-CreER^{T2} (Math1-Cre/-) transgene on a C57BL/6J background were kindly provided by Dr. Rob Machold (New York University). The Math1-Cre transgene expresses Cre recombinase in GCs between embryonic day 13.5 and 16.5 upon activation with tamoxifen (Machold and Fishell, 2005). For experiments involving this transgene, dams carrying E16.5 pups were injected i.p. with 100 mg/kg tamoxifen (Sigma-Aldrich, St. Louis, MO), dissolved in corn oil. Because the tamoxifen injections interfered with parturition, pups were delivered by cesarean section at

E19.5 and cross-fostered to CD-1 dams. All mice were bred at Emory University vivaria, housed on a 12 h light/dark cycle and had access to food and water *ad libitum*. 2–3 week-old mice of both sexes were used for electrophysiological studies. 2–3 month-old mice of both sexes were used for behavioral and anatomical studies. Experiments were in accordance with the Guide for the Care and Use of Laboratory Animals as adopted by the United States National Institutes of Health and Emory University.

PCR was used to genotype mice using the following forward and reverse primers. For the *Cacna1a* knockout allele, 5'-ATAATAAGTCACCTCTCGTTCTAAAG-3' and 5'-CTGACTAGGGGAGGAGTAGAAG-3'; for the flox allele, 5'-ACCTACAGTCTGCCAGGAG-3' and 5'-TGAAGCCCAGACATCCTTGG-3'; for L7-Cre and Math1-Cre alleles, 5'-GCGGTCTGGCAGTAAAAACTATC-3' and 5'-TCTCTGACCAGAGTCATCCTTAGC-3'.

Reverse transcriptase-PCR

Total RNA was isolated from brain using a PureLink RNA kit (Invitrogen, Carlsbad, CA). *Cacna1a* cDNA was synthesized using a Superscript III RT-PCR kit (Invitrogen) with gene-specific primers (5'-AAGTCTCTCCGAGTCCTCC-3' and 5'-TCAGGAGCAGGGAGACAA-3'). Reverse transcriptase-PCR products were sequenced as above to verify the presence of the c.4486T>G mutation.

Western blot

Brain tissue was sonicated in RIPA buffer and the homogenate was centrifuged at 1300 rpm for 10 min. Protein concentration was adjusted and samples were incubated in Laemmli buffer and 4 mM urea at 37°C for 2 hrs. Proteins were separated on a 30% acrylamide gel containing 4M urea, transferred to a blot, and probed with antibodies to the $Ca_V2.1$ α_1 protein (1:200, rabbit polyclonal, Millipore, Billerica, MA) and β-tubulin (1:1000, rabbit polyclonal, Cell Signaling Technology, Danvers, MA) as a loading control. Blots were then incubated with secondary antibody (1:1000, α-rabbit IgG), developed with chemiluminescence, and imaged with a Fuji LAS-3000 digital imager (Fujifilm, Tokyo, Japan).

Electrophysiology

Mice were anesthetized with isoflurane, decapitated and the cerebella quickly removed. Sagittal cerebellar slices (400 μm) were cut on a vibratome and held in Tyrodes solution (in mM: 150 NaCl, 4 KCl, 2 $CaCl_2$, 2 $MgCl_2$, 10 HEPES, 10 glucose, adjusted to pH 7.4 with NaOH) at 34°C for 30 min before allowing them to cool to room temperature. Immediately prior to recording, slices were incubated for 10 min in papain (1 mg/mL, Worthington, Lakewood NJ), dissolved in dissociation solution (in mM: 82 Na_2SO_4, 30 K_2SO_4, 5 $MgCl_2$,10 HEPES, 10 glucose, adjusted to pH 7.4 with NaOH). Slices were then washed in Tyrodes solution, placed in a fresh tube containing 1 mL Tyrodes solution, and dissociated by gentle trituration through a series of fire-polished pipettes. Supernatant containing dissociated cells was placed on poly-L-lysine coated cover slips for electrophysiological recording. Dissociated PCs were readily distinguished from surrounding cells by their large, pear-shaped soma and dendritic stump.

Ba^{2+} currents were recorded in acutely dissociated PCs in whole-cell patch-clamp configuration at room temperature. For voltage-clamp, extracellular solutions were optimized for stable whole-cell recordings of $Ca_V2.1$ currents and contained (in mM): 155 TEA-Cl, 10 HEPES, and 10 $BaCl_2$, adjusted to pH 7.4 with TEA-OH. Prior to recording, TTX (1 μM) was added to the extracellular recording solution to block Na^+ currents. Intracellular solution contained (in mM): 140 Cs Methanesulfonate, 4 $MgCl_2$, 0.5 EGTA, 9 HEPES, 14 creatine phosphate (Tris salt), 4 Mg-ATP, 0.3 Tris-GTP, adjusted to pH 7.4 with CsOH. Electrode resistances in the recording solutions were typically 4–6 MΩ. Reagents used for electrophysiological recordings were obtained from Sigma-Aldrich. Currents were recorded with an Axon Multiclamp amplifier driven by pClamp 10 software (Molecular Devices, Sunnyvale, CA). As soon as the whole-cell patch-clamp configuration was established, Ca^{2+} channel blockers were applied to the extracellular recording solution, which was switched via a Warner fast-exchange bath chamber, and recording protocols were initiated after a 5 min delay. In the case where the contributions of individual Ca^{2+} channel subtypes were measured, antagonists were added sequentially during recordings. Nimodipine (5 μM) was obtained from Sigma-Aldrich. ω-Conotoxin-GVIA (1 μM) and MVIIC (3 μM) were obtained from Ascent Scientific (Princeton, NJ).

Histology

Brains were obtained after transcardial perfusion with saline followed by 4% paraformaldehyde (PFA), post-fixed in 4% PFA and dehydrated and stored in 30% sucrose at 4°C. 30 μm coronal sections of the cerebellum were cut on a freezing microtome and stained with 0.1% Cresyl Violet. To visualize PCs, adjacent sections were reacted with an antibody to calbindin. Endogenous peroxidase activity was quenched with 10% H_2O_2, then blocked with 4% normal goat serum. Tissue was incubated for 48 hrs in primary antibody (1:1000 rabbit polyclonal, Abcam, Cambridge, MA), then for 4 hrs in secondary antibody (1:800 biotinylated α-rabbit, Vector Laboratories, Burlingame, CA), avidin-biotin complex for 2 hrs (Vector Laboratories, Burlingame, CA), then reacted with 3,3-diaminobenzadine (Vector Labs) for 3–5 min. Sections were dehydrated through graded alcohols and xylenes, then mounted and coverslipped.

To assess Cre recombinase activity in L7-Cre and Math1-Cre lines, these lines were bred onto the Rosa26 reporter line, which is permissive for β-Galactosidase expression in the presence of Cre recombinase. Brains were flash-frozen and coronal cryosections were cut at 20 μm. Tissue was incubated in 0.02% Igepal (Sigma-Aldrich), 0.01% sodium deoxycholate, 2 mM $MgCl_2$, 5 mM potassium ferricyanide, 5 mM potassium ferrocyanide and 1 mg/ml 5-Bromo-4-chloro-3-indolyl-β-D-galactopyranoside (X-Gal)(Thermo Fischer Scientific, Waltham, MA) in PBS overnight and counterstained with Nuclear Fast Red (Vector Labs).

Behavioral analysis

Rotarod was used to test coordination. Mice were habituated for 30 seconds to a 4 cm diameter rod (Columbus Instruments, Columbus, OH) rotating at 4 rpm. Rotation speed was increased from 4 to 40 rpm over a 6 min period. Mice that did not fall during the 6 min period were recorded as 6 min. Learning and performance of the task was assessed using the average of 4 consecutive trials over 4 consecutive days. Drug effects were assessed on 3

consecutive trials with mice previously trained on the rotarod. Mice were randomly assigned to drug or vehicle on two consecutive days.

The pole test was used as a second test of motor coordination. Mice were placed with their head oriented upwards on a 50 cm tall, 1 cm diameter vertical pole placed inside their home cage. The time for each mouse to descend and have all four limbs on the cage floor was recorded. Mice performed 5 trials of training each day for 2 days prior to testing. On the test day, mice performed 5 trials and the best time for each mouse was used for analysis.

Photocell activity chambers were used to measure spontaneous locomotor activity. Each mouse was placed in a separate chamber consisting of 20 × 40 cm plexiglass boxes with 4 infrared beams spanning the short axis and 8 infrared beams spanning the long axis (San Diego Instruments, San Diego, CA). Beam breaks were recorded automatically by a computer over a 26 hr time period.

The cling test was used to test strength and agility. Mice were habituated for 1 min on a horizontal 20 × 20 cm framed grid of wire mesh suspended above a padded surface. The frame was then rotated 90° to vertical for 1 min, and then rotated another 90° for 1 min so that the mice were inverted. The time to fall was recorded with a 180 sec cut-off. The average time to fall was determined from 3 trials for each mouse.

Drug challenges were used to test for episodic motor abnormalities. Caffeine (Sigma-Aldrich) was delivered subcutaneously and EtOH was delivered i.p. Both drugs were dissolved in saline and delivered 20 min prior to behavioral testing as previously reported (Fureman et al., 2002).

Data analysis

All data represent the mean ± SEM. For electrophysiological data statistical differences between groups were determined by one-way ANOVA. *I-V* curves were fit with the function: $g(V - E)/(1 + \exp[(V - V_{1/2})/k] + b)$ where g is the maximum conductance, V is the test potential, E is the apparent reversal potential, $V_{1/2}$ is the potential of half activation, k is the slope factor, and b is the baseline. Significant differences between *I-V* curve values were determined with two-way repeated measure ANOVA. For locomotor activity and rotarod data statistical differences between groups were determined by two-way repeated measures ANOVA and Tukey's *post hoc* test. For pole and cling test data statistical differences between groups were determined by oneway ANOVA and Tukey's *post hoc* test.

Results

Verification of the c.4486T>G Cacna1a mutation in EA2 knockin mice

The EA2-causing c.4486T>G mutation was introduced into *Cacna1a* exon 26 by site-directed mutagenesis. After identification of founder lines, the EA2 knockin mutation was confirmed in genomic DNA from unresolved EA2 knockin mice by a series of PCR reactions. A forward primer specific to the *Cacna1a* gene in genomic DNA beyond the 5' end of the knockin construct (P1) was paired with two different reverse primers, one upstream (P2) and one downstream (P3) of the 5' end of a neomycin resistance cassette (Fig.

1A). All mice produced a PCR product with primers P1 and P2, but only mice carrying the knockin construct produced a product with primers P1 and P3 (Fig. 1B). For the 3' end of the construct, a similar strategy was used. Two forward primers, one upstream (P4) and one downstream (P5) of the 3' end of the neomycin resistance cassette, were used with a single reverse primer (P6) to establish that the 3' end of the construct was also inserted properly. Amplification with primers P4 and P6 was only observed in animals with the knockin construct, whereas primers P5 and P6 produced a product in all mice (Fig. 1B). To independently verify the presence of the point mutation, PCR was performed on a short sequence (325 bp) encompassing the c.4486T>G mutation and the results were sequenced (Fig. 1C). Sequencing results matched the long PCR reaction results in all animals tested.

Transcription of the mutant allele was confirmed by sequencing the *Cacna1a* sequence-specific Reverse transcriptase-PCR product obtained using total RNA from EA2/EA2 mouse brain (Fig. 1C). Western blot revealed similar levels of $Ca_V2.1$ α_1 protein in +/+, EA2/+, and EA2/EA2 mouse cerebellum and frontal cortex (Fig. 1D). Thus, the EA2 mutation does not appear to affect transcription or translation *in vivo*, consistent with previous work with this mutation using heterologous expression systems (Jen et al., 2001, Jeng et al., 2006).

$Ca_V2.1$ currents in EA2/EA2 knockin mouse PCs

To characterize the consequences of the EA2 mutation on $Ca_V2.1$ channel function, we performed whole-cell patch clamp recordings of acutely-dissociated PCs from +/+, EA2/+ and EA2/EA2 mice in the presence of $Ca_V1.2$ and $Ca_V2.2$ antagonists. Ca_V3 channels were inactivated by maintaining cells at a holding potential of −60 mV. $Ca_V2.1$ channels normally account for ∼90% of PC somatic Ca^{2+} current (Regan, 1991, Mintz et al., 1992, McDonough et al., 1997). Ba^{2+} current density in EA2/+ mice was reduced by only ∼20% compared to +/+ mice (ANOVA, $F_{2,11}$=2.4; P>0.1; post hoc Tukey's *t*-test, p>0.6). Ba^{2+} current density in EA2/EA2 mice was reduced by ∼70% compared to +/+ mice ($p<0.05$, post hoc Tukey's *t*-test; Fig. 2A and 2B). Thus, when expressed in the mouse, the c.4486T>G mutation results in severely reduced Ca_V currents in cerebellar PCs, in good agreement with findings from studying the human mutation in heterologous expression systems (Jen et al., 2001, Jeng et al., 2006, Jeng et al., 2008).

In EA2 patients and mice expressing hypoconductive $Ca_V2.1$ channel mutants, there is evidence for compensatory upregulation of other Ca^{2+} channel subtypes, which may contribute to pathogenesis (Campbell and Hess, 1999, Qian and Noebels, 2000, Maselli et al., 2003). To assess the differential contribution of $Ca_V2.1$, $Ca_V1.2$ (L-type) and $Ca_V2.2$ (N-type) Ca^{2+} channel subtypes to the whole-cell Ba^{2+} current recorded from EA2/EA2 PCs, we assessed peak Ba^{2+} current following application of Ca_V channel-specific antagonists. Compared to the peak Ba^{2+} current of +/+ PCs, that of EA2/EA2 PCs appeared much more sensitive to the $Ca_V1.2$ channel blocker nimodipine and the $Ca_V2.2$ channel blocker ω-Conotoxin-GVIA (Fig. 2C and 2D). On the other hand, the whole-cell currents in EA2/EA2 PCs were, as expected, much less sensitive to the $Ca_V2.1$ blocker ω-Conotoxin-MVIIC. These data suggest that compensatory increases in non-$Ca_V2.1$ currents accounted for some of the residual whole-cell Ba^{2+} currents conducted through Ca_V channels in EA2/EA2 mouse PCs.

Cerebellar anatomy

Abrogation of $Ca_V2.1$ channel function in *Cacna1a* knockout mice causes profound cerebellar cell death (Jun et al., 1999, Fletcher et al., 2001). Cerebellar degeneration is also present in some, but not all, mutant mouse strains bearing spontaneous *Cacna1a* point mutations (Meier and MacPike, 1971, Herrup and Wilczynski, 1982, Zwingman et al., 2001). Therefore, cerebellar sections from EA2 knockin mice were examined for histopathological signs. No obvious morphological or cytoarchitectural abnormalities were apparent in Nissl-stained cerebellar sections from EA2/+ or EA2/EA2 mice (Fig. 3B, 3D, 3G, and 3I). Furthermore, no evidence of gross PC cell death was observed in sections immunostained for calbindin, which specifically labels cerebellar PCs (Fig. 3L and 3N). These results demonstrate that despite the functional consequences to Ca_V physiology, the EA2-causing p.F1406C (c.4486T>G) mutation does not cause notable cerebellar degeneration in mice.

Effect of EA2 knockin allele number on baseline motor function

Ataxic attacks in EA2 patients are superimposed on a relatively normal neurological baseline. Despite the reduction in $Ca_V2.1$ channel function, EA2/+ and EA2/EA2 knockin mice had no obvious motor abnormalities at baseline. Nonetheless, motor function was quantitatively assessed using a battery of standard motor-behavioral assays. Because there was evidence for a gene dose effect of the EA2 knockin mutation on Ca_V physiology, we tested whether gene dose also affected motor function by generating mice that carry one EA2 *Cacna1a* allele and one knockout allele (EA2/−); +/− mice were also tested to control for the knockout allele.

Coordination assessed by accelerating rotarod revealed a significant effect of genotype (ANOVA; $F_{4,60}=9.12$, $P<0.001$; Fig. 4A). *Post hoc* analysis showed that time to fall for EA2/− mice was significantly shorter than +/+ ($p<0.001$), +/− ($p<0.001$), EA2/+ ($p<0.01$), and EA2/EA2 mice ($p=0.001$). +/−, EA2/+, and EA2/EA2 mice did not differ from each other or +/+ mice. There was a significant effect of test day ($F_{3180}=90.0$, $P<0.001$), whereby rotarod performance improved over the four test days across all genotypes. There was no genotype x day interaction effect ($F_{12,180}=1.72$, $P>0.05$), suggesting that despite the overall defect in rotarod performance, EA2/− mice exhibited significant motor learning across test days.

Climbing ability was assessed using the pole test, which measures the time for a mouse placed nose up at the top of a vertical pole to turn and descend to the cage floor. A significant genotype effect was observed ($F_{4,43}=3.49$, $P<0.05$; Fig. 4B), whereby EA2/− mice were significantly slower in reaching the cage floor than +/+ and +/− ($p<0.05$), but there was no significant difference between EA2/EA2 and EA2/− mice, reflecting a non-significant trend toward slower performance in EA2/EA2 mice compared to +/+, +/− and EA2/+ mice.

Performances on the accelerating rotarod and pole test are dependent on strength and volitional movement as well as coordination and skilled movement. Therefore, we also tested for these confounds in EA2 knockin mice. No effect of genotype was observed in the

cling test ($F_{4,44}$=0.27, P>0.5; Fig. 4C), which measures the time to fall from a framed grid of wire mesh that is rotated 90° to vertical for 1 min, and then rotated another 90° for 1 min so that the mice were inverted. We also tested spontaneous locomotor activity in a 24 hr period using photoactivity chambers. No effect of genotype was observed in locomotor activity ($F_{4,27}$=0.97, P>0.4; Fig. 4D). Overall, results from the motor-behavioral assays suggest an effect of the EA2 knockin allele number on coordinated and skilled movements, rather than effects on strength or volitional movement. Moreover, the motor deficits exhibited by EA2/− mice on the accelerating rotarod and pole test were not associated with notable cerebellar pathology (Fig. 3E, 3J, and 3O), suggesting that the cause may be related to deficits in $Ca_V2.1$ channel function rather than degeneration.

Triggers of episodic dysfunction in EA2/EA2 or EA2/− mice

Ataxic attacks in EA2 patients are typically triggered by caffeine, EtOH, and stress (Griggs and Nutt, 1995, Gordon, 1998, Denier et al., 1999, Jen, 1999, Bhatia et al., 2000). We have previously shown that caffeine, EtOH, and stress reliably trigger attacks in the spontaneous *Cacna1a* mouse mutant *tottering* (Fureman et al., 2002), demonstrating that episodic attacks of neurological dysfunction caused by *Cacna1a* mutations can be induced in mice. Because we expected attacks of ataxia in mice carrying the EA2 allele, we used performance on the accelerating rotarod as an objective measure of motor incoordination elicited or exacerbated by triggers of attacks. These studies used mice previously trained on the rotarod to dissociate motor performance from motor learning. +/+, EA2/+, EA2/EA2, and EA2/− mice were challenged with 15 mg/kg caffeine, which reliably causes attacks in 95% of *tottering* mice (Fureman et al., 2002). There was no effect of genotype ($F_{3,38}$=1.41, P>0.2), drug ($F_{1,38}$=0.24, P>0.5), or genotype × drug interaction ($F_{3,38}$=0.82, P>0.4; Fig. 5A). We also challenged the mice with EtOH, which dose-dependently elicits attacks in *tottering* mice (Fureman et al., 2002). A genotype effect was observed ($F_{3,38}$=4.73, P<0.01) and *post hoc* analysis showed that EA2/− mice had a significantly reduced performance across all the doses of EtOH (p<0.05). Furthermore, a drug effect was observed ($F_{3,114}$=167, P<0.001), indicating that EtOH caused reduced performance on the rotarod, as expected. An interaction between drug and genotype, however, was not observed ($F_{9,114}$=0.66, P>0.5), indicating that all genotypes were similarly affected (Fig. 5B). Although increasing doses of EtOH increasingly impaired performance, at no point was any genotype grossly affected and at no time were there precipitous changes in motor function suggestive of sudden onset of ataxia or any other type of paroxysmal neurological dysfunction.

Effect of isolating the EA2/− genotype to either PCs or GCs on motor performance

Mice carrying the EA2 allele paired with the knockout allele exhibit poor motor performance but heterozygotes that carry the EA2 allele paired with the normal allele are motorically normal. We therefore exploited this genotype/phenotype relationship to determine if abnormal PCs were the major determinants of the ataxia associated with the EA2 allele. We have demonstrated that selective elimination of $Ca_V2.1$ channels within PCs causes ataxia (Todorov et al., 2012) by breeding the L7-Cre transgene, which expresses Cre recombinase in postnatal PCs, onto the floxed *Cacna1a* mouse strain (flox/flox). Therefore, we used a conditional approach to isolate the ataxia-causing genotype to PCs by breeding the L7-Cre transgene onto EA2/flox mice, creating mice that expressed only the EA2 allele

in PCs, but in all other cells, the mice were heterozygous with one normoactive allele and one EA2 allele (EA2/flox; L7-Cre/-). These mice expressed Cre specifically in PCs (Fig. 6A). We assessed motor learning and performance in these mice with the rotarod. Additionally, EA2/+ mice carrying the L7-Cre transgene (EA2/+; L7-Cre/-) were tested to control for the effects of Cre recombinase expression within PCs, and EA2/flox mice were tested to control for the presence of the floxed allele (See Table 1 for details). Surprisingly, no effect of genotype was observed ($F_{2,23}$=0.17, P>0.5; Fig. 7A). Within subjects analysis showed a significant main effect of day ($F_{3,69}$=4.91, P<0.01) but no interaction between genotype and day ($F_{6,69}$=0.66, P>0.5), suggesting that the different genotypes improved rotarod performance at a similar rate. These results were replicated using an independent second group of mice (not shown).

Next, we use a similar strategy to determine whether the EA2/− genotype confined to GCs was sufficient to cause the motor dysfunction. In this experiment, the Math1-Cre transgene was used to drive Cre recombinase activity specifically in GCs (Machold and Fishell, 2005) (Fig. 6B). We bred the Math1-Cre transgene onto EA2/flox mice, creating mice that expressed only the EA2 allele in GCs, but in all other cells, the mice were heterozygous with one normoactive allele and one EA2 allele (EA2/flox; Math1-Cre/-). We tested these mice and EA2/+ carrying Math1-Cre (EA2/+; Math1-Cre/-) and EA2/flox littermates as controls on the accelerating rotarod, similar to the strategy described above for PCs. No effect of genotype was observed ($F_{2,36}$=0.84, P>0.25; Fig. 7B). An effect of day ($F_{3,108}$=26.6, P<0.001) and an interaction between day and genotype were observed ($F_{6,108}$=5.15, P<0.001). *Post hoc* analysis revealed that EA2/flox mice had reduced performance relative to EA2/flox; Math1-Cre/- and EA2/+; Math1-Cre/- (p<0.01) only on day 3 of testing. It is unlikely that the Math1-Cre transgene conferred any advantage specific to the test day.

Discussion

Here, we characterized the first genetic mouse model of EA2. Our knockin mouse carries a point mutation in *Cacna1a* that causes a ∼70% reduction in the Ca^{2+} current of dissociated PCs when bred as homozygotes. It was surprising that motor function, assayed by multiple tests, was relatively normal in homozygous mutant EA2/EA2 mice. Furthermore, common triggers, e.g. caffeine and EtOH, which bring about episodic motor dysfunction in *tottering* mice and EA2 patients did not elicit such dysfunction in EA2 knockin mice.

The lack of a measurable motor phenotype in EA2/EA2 mice is puzzling when the biophysical effects of the p.F1406C (c.4486T>G) missense mutation are compared to the biophysical properties of other recessive *Cacna1a* mutant lines. *Tottering*, *rocker*, and *rolling Nagoya* mice all carry spontaneous missense mutations in *Cacna1a* and homozygotes of these strains all exhibit a clear neurobehavioral phenotype that includes cerebellar ataxia and paroxysmal dystonia (Oda, 1973, Shirley et al., 2008). *Leaner* mice that carry a *Cacna1a* nonsense truncation mutation (Meier and MacPike, 1971, Fletcher et al., 1996) which results in a 40–60% reduction in the PC $Ca_V2.1$ Ca^{2+} current similar to the reduction in current measured in EA2/EA2 mouse PCs (Dove et al., 1998, Wakamori et al., 1998), suffer from a severe phenotype with chronic dystonia similar to the severe phenotype observed in *Cacna1a* knockout mice. The phenotypic variability may be, in part, explained

by the complex transcription associated with the *Cacna1a* gene itself. Not only does *Cacna1a* mRNA undergo alternative splicing to encode the 'P-type' and 'Q-type' channels (Bourinet et al., 1999), the mRNA is also bicistronic with the first cistron expressing the $Ca_V2.1$ channel, and the second expressing a transcription factor, which is independent of channel function (Du et al., 2013). The *Cacna1a*–encoded transcription factor mediates Purkinje cell development and expression of the transcription factor is sufficient to restore, in part, the behavioral phenotype of *Cacna1a* knockout mice, so it is not surprising that postnatal knockdowns are dissimilar to knockout mice. Genomic mutations may alter the three dimensional conformation of the mRNA to specifically disrupt translation of the transcription factor, which might explain phenotypic divergence despite comparable deficits in channel function. Additionally or alternatively, the relatively mild EA2/EA2 phenotype might be explained by adaptive changes that compensate for the reduced $Ca_V2.1$ current. Indeed, we showed that EA2/EA2 PCs exhibit compensatory increases in $Ca_V1.2$ and $Ca_V2.2$ currents. Our group and others have shown that specific, maladaptive changes to $Ca_V1.2$ function, as well as other membrane ion channels contribute to motor dysfunction in *tottering* mice (Campbell and Hess, 1999, Weisz et al., 2005, Erickson et al., 2007, Alvina and Khodakhah, 2010a, b), though further research is needed to determine the relevance of these channels to behavioral compensation in EA2/EA2 mice.

Pairing the EA2 allele with the knockout allele was, however, sufficient to cause motor dysfunction. EA2/− mice exhibit a phenotype intermediate to +/− mice, which exhibit no measurable phenotype, and −/− mice, which exhibit a very severe phenotype of chronic dystonia and early lethality (Jun et al., 1999, Fletcher et al., 2001). Thus the EA2/− mice clearly demonstrate that the EA2 allele does have a deleterious effect on motor function. The phenotype of EA2/− mice is most conservatively described as a reduction in performance on coordinated and skilled motor tasks, though the most likely cause of this reduction is ataxia. Reduced motor performance in these mice is not associated with overt cell loss in the cerebellum unlike in *leaner* mice or −/− mice, which exhibit profound neuronal loss throughout the cerebellum (Herrup and Wilczynski, 1982, Jun et al., 1999, Fletcher et al., 2001, Todorov et al., 2012). In EA2/− mice, the motor deficit apparently results from dysfunction, not degeneration. Further research is needed to determine if the ataxic phenotype of EA2/− mice results from further (>70%) reduction in $Ca_V2.1$ current, maladaptive changes in other ion channels, or both. For this, a multidisciplinary approach involving both *ex vivo* physiology and behavioral testing would be required to truly ascribe a molecular mechanism to the phenotype of EA2/− mice.

We explored the cell type-specific contributions to the motor deficit by using conditional genetics to confine the EA2/− genotype exclusively to either PCs or GCs. Isolating the EA2/- genotype to GCs was not sufficient to elicit a motor phenotype. This result was not entirely surprising in light of the results from GC-specific *Cacna1a* knockouts, which exhibit subtle phenotypes. One group showed that knockout of *Cacna1a* in most GCs causes only a subtle deficit in rotarod performance but a profound effect on the consolidation of learning of complex motor tasks (Galliano et al., 2013). Another group, however, showed that GC-specific *Cacna1a* knockouts exhibited a phenotype similar to *tottering* mice with baseline ataxia and paroxysmal dyskinesia, though this was only true in only ∼25% of mice

with this genotype (Maejima et al., 2013). Here, the resulting cerebellar dysfunction is likely sub-threshold for eliciting behavioral dysfunction for two reasons. First, based on Figure 6, it is possible that recombination did not occur in all GCs, similar to the work of Galliano and colleagues (2013). Second, even if recombination occurred in all GCs, these cells still retain some residual $Ca_V2.1$ channel current, which may abrogate the subtle phenotypes observed in the complete GC knockouts.

It was surprising that isolating the EA2/- genotype to PCs was not sufficient to elicit overt motor dysfunction. We have previously shown that restricting the *tottering* mouse genotype to PCs causes ataxia and episodic dystonia, similar to the phenotype observed in *tottering* mice (Raike et al., 2012). Additionally, selective postnatal knockdown of *Cacna1a* in PCs using L7-Cre also caused overt motor defects. In one study, selective postnatal knockdown of *Cacna1a* in PCs caused ataxia, whereas in the other study, the mice recapitulated the *tottering* mouse phenotype (Mark et al., 2011, Todorov et al., 2012). Thus, effects of postnatal knockdown can be quite variable. There are several explanations for the lack of motor dysfunction in the EA2/flox; L7-Cre/- mice compared to EA2/- mice. First, in EA2/- mice, the *Cacna1a*-encoded transcription factor, which regulates PC development, is disrupted throughout development. In contrast, the transcription factor remains intact in EA2/flox; L7-Cre/- mice until after birth. The same is true for the normal ‘floxed’ channel. Second, residual $Ca_V2.1$ channel current conducted by the EA2 mutant protein or possible compensatory up-regulation of other channel subtypes is adequate to maintain PC function. Third, the motor dysfunction observed in EA2/- is not due to dysfunction of PCs alone. It is possible that the concurrent albeit subtle abnormalities of both PCs and GCs *together* may mediate the ataxia in EA2/- mice or that the dysfunction in EA2/- mice originates from cell types outside of the cerebellum. Though *Cacna1a* is most abundantly expressed in cerebellum, other brain regions relevant for movement such as motor cortex and basal ganglia show expression as well (Lein et al., 2007). This scenario cannot be ruled out, but is not supported by data from other *Cacna1a* mutants where cerebellar circuitry is specifically implicated in behavioral dysfunction (Campbell et al., 1999, Walter et al., 2006, Raike et al., 2012). Fourth, the dysfunctional signaling occurs downstream of GCs and PCs in deep cerebellar nuclei, which also express $Ca_V2.1$ channels. The deep cerebellar nuclei integrate information from PCs and provide the efferents from the cerebellum. Abnormal deep cerebellar nuclei signaling may override other cerebellar signals or even augment the abnormal signals sent by PCs. Fifth, background strains differ, with EA2/flox; L7-Cre/- mice inbred on C57BL6/J but EA2/- on a mixed background that is predominantly C57BL. Finally, technical limitations of Cre-flox genetics should be considered. Although both the L7-Cre and Math1-Cre lines produce robust Cre recombinase activity in PCs and GCs, respectively (Barski et al., 2000, Machold and Fishell, 2005) and several studies, including our own, have illustrated motor behavioral effects of Cre mediated recombination of floxed *Cacna1a* in PCs and GCs (Mark et al., 2011, Raike et al., 2012, Todorov et al., 2012, Galliano et al., 2013, Maejima et al., 2013, Raike et al., 2013), it is possible that recombination was inadequate. Indeed, others have reported that in another mouse line carrying the L7-Cre transgene, only 52% of Purkinje cells exhibited Cre mediated excision of the gene of interest (Furrer et al., 2011).

Additional work is needed to delineate the cell type(s) involved in ataxic disorders. In the case of this model and perhaps other ataxias, dysfunction of two or more neuronal subtypes may be necessary for the expression of abnormal movement. This hypothesis has important implications for the treatment of ataxias, which largely focuses on altering PC physiology (Strupp et al., 2004, Jen et al., 2007, Strupp et al., 2007), suggesting that it may be useful to broaden the approach to include other cerebellar cell types.

Acknowledgments

This work was supported by the United States National Institute of Health (NS058596, NS33592, T32GM08605, T32NS007480). We thank Dr. David Yue for the *Cacna1a* knockout mice and Dr. Rob Machold for the Math1-Cre mice.

References

Alvina K, Khodakhah K. KCa channels as therapeutic targets in episodic ataxia type-2. J Neurosci. 2010a; 30:7249–7257. [PubMed: 20505091]

Alvina K, Khodakhah K. The therapeutic mode of action of 4-aminopyridine in cerebellar ataxia. J Neurosci. 2010b; 30:7258–7268. [PubMed: 20505092]

Baloh RW. Episodic ataxias 1 and 2. Handb Clin Neurol. 2012; 103:595–602. [PubMed: 21827920]

Barski JJ, Dethleffsen K, Meyer M. Cre recombinase expression in cerebellar Purkinje cells. Genesis. 2000; 28:93–98. [PubMed: 11105049]

Bhatia KP, Griggs RC, Ptacek LJ. Episodic movement disorders as channelopathies. Mov Disord. 2000; 15:429–433. [PubMed: 10830404]

Bourinet E, Soong TW, Sutton K, Slaymaker S, Mathews E, Monteil A, Zamponi GW, Nargeot J, Snutch TP. Splicing of alpha 1A subunit gene generates phenotypic variants of P-and Q-type calcium channels. Nat Neurosci. 1999; 2:407–415. [PubMed: 10321243]

Campbell DB, Hess EJ. L-type calcium channels contribute to the tottering mouse dystonic episodes. Mol Pharmacol. 1999; 55:23–31. [PubMed: 9882694]

Campbell DB, North JB, Hess EJ. Tottering mouse motor dysfunction is abolished on the Purkinje cell degeneration (pcd) mutant background. Exp Neurol. 1999; 160:268–278. [PubMed: 10630211]

Denier C, Ducros A, Vahedi K, Joutel A, Thierry P, Ritz A, Castelnovo G, Deonna T, Gerard P, Devoize JL, Gayou A, Perrouty B, Soisson T, Autret A, Warter JM, Vighetto A, Van Bogaert P, Alamowitch S, Roullet E, Tournier-Lasserve E. High prevalence of CACNA1A truncations and broader clinical spectrum in episodic ataxia type 2. Neurology. 1999; 52:1816–1821. [PubMed: 10371528]

Diener HC, Dichgans J. Pathophysiology of cerebellar ataxia. Mov Disord. 1992; 7:95–109. [PubMed: 1584245]

Dove LS, Abbott LC, Griffith WH. Whole-cell and single-channel analysis of P-type calcium currents in cerebellar Purkinje cells of leaner mutant mice. J Neurosci. 1998; 18:7687–7699. [PubMed: 9742139]

Du X, Wang J, Zhu H, Rinaldo L, Lamar KM, Palmenberg AC, Hansel C, Gomez CM. Second cistron in CACNA1A gene encodes a transcription factor mediating cerebellar development and SCA6. Cell. 2013; 154:118–133. [PubMed: 23827678]

Erickson MA, Haburcak M, Smukler L, Dunlap K. Altered functional expression of Purkinje cell calcium channels precedes motor dysfunction in tottering mice. Neuroscience. 2007; 150:547–555. [PubMed: 18023294]

Feddersen RM, Ehlenfeldt R, Yunis WS, Clark HB, Orr HT. Disrupted cerebellar cortical development and progressive degeneration of Purkinje cells in SV40 T antigen transgenic mice. Neuron. 1992; 9:955–966. [PubMed: 1419002]

Fletcher CF, Lutz CM, O'Sullivan TN, Shaughnessy JD Jr. Hawkes R, Frankel WN, Copeland NG, Jenkins NA. Absence epilepsy in tottering mutant mice is associated with calcium channel defects. Cell. 1996; 87:607–617. [PubMed: 8929530]

Fletcher CF, Tottene A, Lennon VA, Wilson SM, Dubel SJ, Paylor R, Hosford DA, Tessarollo L, McEnery MW, Pietrobon D, Copeland NG, Jenkins NA. Dystonia and cerebellar atrophy in Cacna1a null mice lacking P/Q calcium channel activity. FASEB J. 2001; 15:1288–1290. [PubMed: 11344116]

Fureman BE, Jinnah HA, Hess EJ. Triggers of paroxysmal dyskinesia in the calcium channel mouse mutant tottering. Pharmacol Biochem Behav. 2002; 73:631–637. [PubMed: 12151038]

Furrer SA, Mohanachandran MS, Waldherr SM, Chang C, Damian VA, Sopher BL, Garden GA, La Spada AR. Spinocerebellar ataxia type 7 cerebellar disease requires the coordinated action of mutant ataxin-7 in neurons and glia, and displays non-cell-autonomous bergmann glia degeneration. J Neurosci. 2011; 31:16269–16278. [PubMed: 22072678]

Galliano E, Gao Z, Schonewille M, Todorov B, Simons E, Pop AS, D'Angelo E, van den Maagdenberg AM, Hoebeek FE, De Zeeuw CI. Silencing the majority of cerebellar granule cells uncovers their essential role in motor learning and consolidation. Cell Rep. 2013; 3:1239–1251. [PubMed: 23583179]

Gordon N. Episodic ataxia and channelopathies. Brain Dev. 1998; 20:9–13. [PubMed: 9533553]

Griggs RC, Nutt JG. Episodic ataxias as channelopathies. Ann Neurol. 1995; 37:285–287. [PubMed: 7535034]

Herrup K, Wilczynski SL. Cerebellar cell degeneration in the leaner mutant mouse. Neuroscience. 1982; 7:2185–2196. [PubMed: 7145091]

Holmes G. The symptoms of acute cerebellar injuries due to gunshot injuries. Brain. 1917; 40:461–535.

Imbrici P, Eunson LH, Graves TD, Bhatia KP, Wadia NH, Kullmann DM, Hanna MG. Late-onset episodic ataxia type 2 due to an in-frame insertion in CACNA1A. Neurology. 2005; 65:944–946. [PubMed: 16186543]

Imbrici P, Jaffe SL, Eunson LH, Davies NP, Herd C, Robertson R, Kullmann DM, Hanna MG. Dysfunction of the brain calcium channel CaV2.1 in absence epilepsy and episodic ataxia. Brain. 2004; 127:2682–2692. [PubMed: 15483044]

Jen J. Calcium channelopathies in the central nervous system. Curr Opin Neurobiol. 1999; 9:274–280. [PubMed: 10395579]

Jen J, Wan J, Graves M, Yu H, Mock AF, Coulin CJ, Kim G, Yue Q, Papazian DM, Baloh RW. Loss-of-function EA2 mutations are associated with impaired neuromuscular transmission. Neurology. 2001; 57:1843–1848. [PubMed: 11723274]

Jen JC, Graves TD, Hess EJ, Hanna MG, Griggs RC, Baloh RW. Primary episodic ataxias: diagnosis, pathogenesis and treatment. Brain. 2007; 130:2484–2493. [PubMed: 17575281]

Jeng C, Chen Y, Chen Y, Tang C. Dominant-Negative Effects of Human P/Q-type Ca2+ Channel Mutations Associated with Episodic Ataxia Type 2. American Journal of Cell Physiology. 2006; 290:1209–1220.

Jeng CJ, Sun MC, Chen YW, Tang CY. Dominant-negative effects of episodic ataxia type 2 mutations involve disruption of membrane trafficking of human P/Q-type Ca2+ channels. J Cell Physiol. 2008; 214:422–433. [PubMed: 17654512]

Jun K, Piedras-Renteria ES, Smith SM, Wheeler DB, Lee SB, Lee TG, Chin HM, Adams ME, Scheller RH, Tsien RW, Shin HS. Ablation of P/Q-type Ca2+ channel currents, altered synaptic transmission, and progressive ataxia in mice lacking the alpha(1A)-subunit. Proceedings of the National Academy of Sciences of the United States of America. 1999; 96:15245–15250. [PubMed: 10611370]

Kodama T, Itsukaichi-Nishida Y, Fukazawa Y, Wakamori M, Miyata M, Molnar E, Mori Y, Shigemoto R, Imoto K. A CaV2.1 calcium channel mutation rocker reduces the number of postsynaptic AMPA receptors in parallel fiber-Purkinje cell synapses. Eur J Neurosci. 2006; 24:2993–3007. [PubMed: 17156361]

Lein ES, Hawrylycz MJ, Ao N, Ayres M, Bensinger A, Bernard A, Boe AF, Boguski MS, Brockway KS, Byrnes EJ, Chen L, Chen L, Chen TM, Chin MC, Chong J, Crook BE, Czaplinska A, Dang CN, Datta S, Dee NR, Desaki AL, Desta T, Diep E, Dolbeare TA, Donelan MJ, Dong HW, Dougherty JG, Duncan BJ, Ebbert AJ, Eichele G, Estin LK, Faber C, Facer BA, Fields R, Fischer SR, Fliss TP, Frensley C, Gates SN, Glattfelder KJ, Halverson KR, Hart MR, Hohmann JG,

Howell MP, Jeung DP, Johnson RA, Karr PT, Kawal R, Kidney JM, Knapik RH, Kuan CL, Lake JH, Laramee AR, Larsen KD, Lau C, Lemon TA, Liang AJ, Liu Y, Luong LT, Michaels J, Morgan JJ, Morgan RJ, Mortrud MT, Mosqueda NF, Ng LL, Ng R, Orta GJ, Overly CC, Pak TH, Parry SE, Pathak SD, Pearson OC, Puchalski RB, Riley ZL, Rockett HR, Rowland SA, Royall JJ, Ruiz MJ, Sarno NR, Schaffnit K, Shapovalova NV, Sivisay T, Slaughterbeck CR, Smith SC, Smith KA, Smith BI, Sodt AJ, Stewart NN, Stumpf KR, Sunkin SM, Sutram M, Tam A, Teemer CD, Thaller C, Thompson CL, Varnam LR, Visel A, Whitlock RM, Wohnoutka PE, Wolkey CK, Wong VY, Wood M, Yaylaoglu MB, Young RC, Youngstrom BL, Yuan XF, Zhang B, Zwingman TA, Jones AR. Genome-wide atlas of gene expression in the adult mouse brain. Nature. 2007; 445:168–176. [PubMed: 17151600]

Machold R, Fishell G. Math1 is expressed in temporally discrete pools of cerebellar rhombic-lip neural progenitors. Neuron. 2005; 48:17–24. [PubMed: 16202705]

Maejima T, Wollenweber P, Teusner LU, Noebels JL, Herlitze S, Mark MD. Postnatal loss of P/Q-type channels confined to rhombic-lip-derived neurons alters synaptic transmission at the parallel fiber to purkinje cell synapse and replicates genomic Cacna1a mutation phenotype of ataxia and seizures in mice. J Neurosci. 2013; 33:5162–5174. [PubMed: 23516282]

Mark MD, Maejima T, Kuckelsberg D, Yoo JW, Hyde RA, Shah V, Gutierrez D, Moreno RL, Kruse W, Noebels JL, Herlitze S. Delayed postnatal loss of P/Q-type calcium channels recapitulates the absence epilepsy, dyskinesia, and ataxia phenotypes of genomic Cacna1a mutations. J Neurosci. 2011; 31:4311–4326. [PubMed: 21411672]

Maselli RA, Wan J, Dunne V, Graves M, Baloh RW, Wollmann RL, Jen J. Presynaptic failure of neuromuscular transmission and synaptic remodeling in EA2. Neurology. 2003; 61:1743–1748. [PubMed: 14694040]

McDonough SI, Mintz IM, Bean BP. Alteration of P-type calcium channel gating by the spider toxin omega-Aga-IVA. Biophys J. 1997; 72:2117–2128. [PubMed: 9129813]

Meier H, MacPike AD. Three syndromes produced by two mutant genes in the mouse. Clinical, pathological, and ultrastructural bases of tottering, leaner, and heterozygous mice. J Hered. 1971; 62:297–302. [PubMed: 4941467]

Mezghrani A, Monteil A, Watschinger K, Sinnegger-Brauns MJ, Barrere C, Bourinet E, Nargeot J, Striessnig J, Lory P. A destructive interaction mechanism accounts for dominant-negative effects of misfolded mutants of voltage-gated calcium channels. J Neurosci. 2008; 28:4501–4511. [PubMed: 18434528]

Mintz IM, Venema VJ, Swiderek KM, Lee TD, Bean BP, Adams ME. P-type calcium channels blocked by the spider toxin omega-Aga-IVA. Nature. 1992; 355:827–829. [PubMed: 1311418]

Oda S. The observation of rolling mouse Nagoya (rol), a new neurological mutant, and its maintenance (author's transl). Jikken Dobutsu. 1973; 22:281–288. [PubMed: 4799944]

Pietrobon D. CaV2.1 channelopathies. Pflugers Arch. 2010; 460:375–393. [PubMed: 20204399]

Qian J, Noebels JL. Presynaptic Ca(2+) influx at a mouse central synapse with Ca(2+) channel subunit mutations. J Neurosci. 2000; 20:163–170. [PubMed: 10627593]

Raike RS, Kordasiewicz HB, Thompson RM, Gomez CM. Dominant-negative suppression of Cav2.1 currents by alpha(1)2.1 truncations requires the conserved interaction domain for beta subunits. Mol Cell Neurosci. 2007; 34:168–177. [PubMed: 17161621]

Raike RS, Pizoli CE, Weisz C, van den Maagdenberg AM, Jinnah HA, Hess EJ. Limited regional cerebellar dysfunction induces focal dystonia in mice. Neurobiol Dis. 2012; 49C:200–210. [PubMed: 22850483]

Raike RS, Weisz C, Hoebeek FE, Terzi MC, De Zeeuw CI, van den Maagdenberg AM, Jinnah HA, Hess EJ. Stress, caffeine and ethanol trigger transient neurological dysfunction through shared mechanisms in a mouse calcium channelopathy. Neurobiol Dis. 2013; 50:151–159. [PubMed: 23009754]

Rajakulendran S, Kaski D, Hanna MG. Neuronal P/Q-type calcium channel dysfunction in inherited disorders of the CNS. Nat Rev Neurol. 2012; 8:86–96. [PubMed: 22249839]

Randall A, Tsien RW. Pharmacological Dissection of Multiple Types of Ca2+ Channel Currents in Rat Cerebellar Granule Neurons. Journal of Neuroscience. 1995; 15:2995–3012. [PubMed: 7722641]

Regan LJ. Voltage-dependent calcium currents in Purkinje cells from rat cerebellar vermis. J Neurosci. 1991; 11:2259–2269. [PubMed: 1712382]

Shirley TL, Rao LM, Hess EJ, Jinnah HA. Paroxysmal dyskinesias in mice. Mov Disord. 2008; 23:259–264. [PubMed: 17999434]

Strupp M, Kalla R, Dichgans M, Freilinger T, Glasauer S, Brandt T. Treatment of episodic ataxia type 2 with the potassium channel blocker 4-aminopyridine. Neurology. 2004; 62:1623–1625. [PubMed: 15136697]

Strupp M, Zwergal A, Brandt T. Episodic ataxia type 2. Neurotherapeutics. 2007; 4:267–273. [PubMed: 17395137]

Todorov B, Kros L, Shyti R, Plak P, Haasdijk ED, Raike RS, Frants RR, Hess EJ, Hoebeek FE, De Zeeuw CI, van den Maagdenberg AM. Purkinje cell-specific ablation of Cav2.1 channels is sufficient to cause cerebellar ataxia in mice. Cerebellum. 2012; 11:246–258. [PubMed: 21870131]

Todorov B, van de Ven RC, Kaja S, Broos LA, Verbeek SJ, Plomp JJ, Ferrari MD, Frants RR, van den Maagdenberg AM. Conditional inactivation of the Cacna1a gene in transgenic mice. Genesis. 2006; 44:589–594. [PubMed: 17146767]

Tomlinson SE, Hanna MG, Kullmann DM, Tan SV, Burke D. Clinical neurophysiology of the episodic ataxias: insights into ion channel dysfunction in vivo. Clin Neurophysiol. 2009; 120:1768–1776. [PubMed: 19734086]

Wakamori M, Yamazaki K, Matsunodaira H. Single tottering mutations responsible for the neuropathic phenotype of the P-type calcium channel. Journal of Biological Chemistry. 1998; 52:34857–34867. [PubMed: 9857013]

Walter JT, Alvina K, Womack MD, Chevez C, Khodakhah K. Decreases in the precision of Purkinje cell pacemaking cause cerebellar dysfunction and ataxia. Nat Neurosci. 2006; 9:389–397. [PubMed: 16474392]

Wappl E, Koschak A, Poteser M, Sinnegger MJ, Walter D, Eberhart A, Groschner K, Glossmann H, Kraus RL, Grabner M, Striessnig J. Functional consequences of P/Q-type Ca2+ channel Cav2.1 missense mutations associated with episodic ataxia type 2 and progressive ataxia. J Biol Chem. 2002; 277:6960–6966. [PubMed: 11742003]

Weisz CJ, Raike RS, Soria-Jasso LE, Hess EJ. Potassium channel blockers inhibit the triggers of attacks in the calcium channel mouse mutant tottering. J Neurosci. 2005; 25:4141–4145. [PubMed: 15843617]

Zwingman TA, Neumann PE, Noebels JL, Herrup K. Rocker is a new variant of the voltage-dependent calcium channel gene Cacna1a. J Neurosci. 2001; 21:1169–1178. [PubMed: 11160387]

Highlights

1. The first genetic mouse model of episodic ataxia type 2 (EA2) was created.
2. The *Cacna1a* gene mutation causes $Ca_V2.1$ channel hypoconductance.
3. Motor deficits in the mice were surprisingly subtle.
4. Purkinje cells nor cerebellar granule cells, alone, drove the motor deficits.

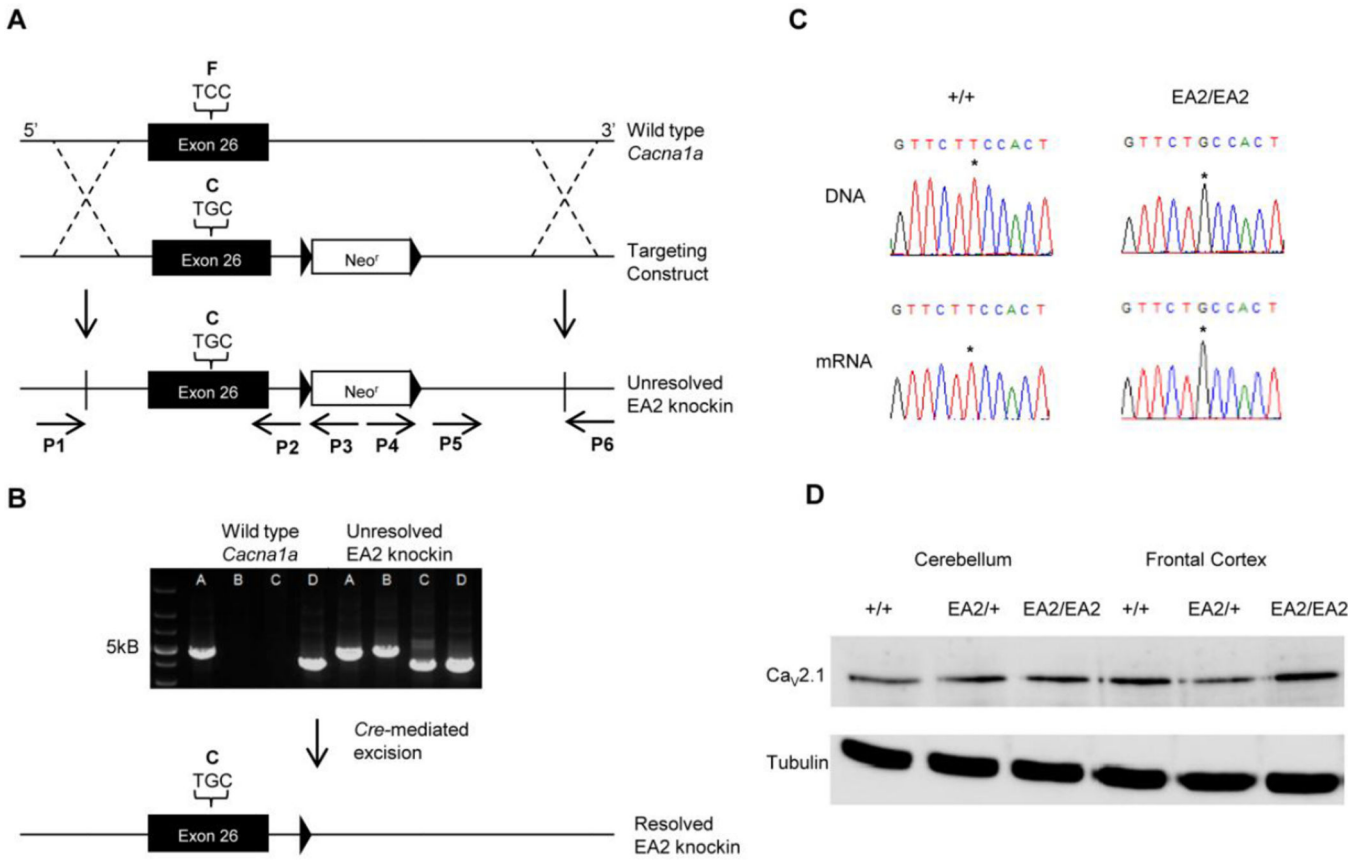

Fig. 1.

Generation and molecular characterization of EA2 knockin mice. (A) The EA2 knockin construct contained a c.4486T>G substitution, coding a p.F1406C missense in exon 26 of *Cacna1a* and a neomycin resistance cassette (neo^r), flanked by two loxP sites, upstream of exon 27. The targeting construct was introduced into C57BL/6J–derived ES cells via homologous recombination and cells carrying the construct were injected into blastocysts. (B) A series of PCRs from the DNA of F1 mice were used to verify correct homologous recombination. Reactions from primers P1 and P3 illustrate proper insertion of the 5' end of the construct and reactions from primers P4 and P6 verify 3' recombination. (C) DNA and mRNA sequences illustrate the presence of the c.4486T>G substitution in the PCR product of genomic DNA and RT-PCR product of brain mRNA from +/+ and EA2/EA2 mice. (D) Western blot shows the normal expression of $Ca_V2.1$ in frontal cortex and cerebellum.

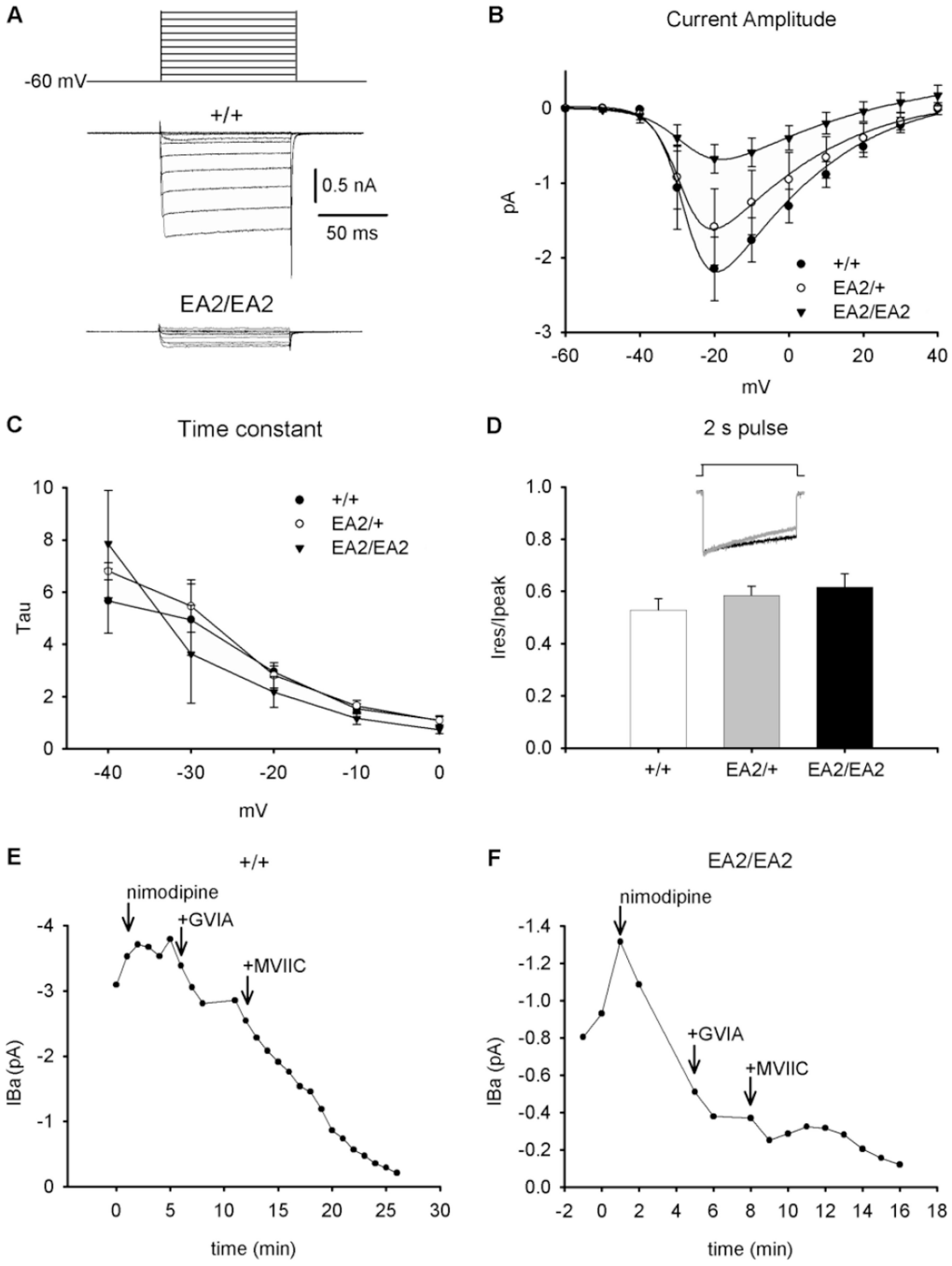

Fig. 2.

Physiological properties of EA2 knockin (p.F1406C) $Ca_V2.1$ (A) Depolarizing voltage pulses (100 ms) ranging from −60 to + 40 mV (top) were applied to acutely dissociated PCs in the presence of $Ca_V1.2$ and $Ca_V2.2$ antagonists, and Ba^{2+} currents (I_{Ba}) were measured. Representative traces from +/+ and EA2/EA2 mice are shown (bottom). (B) Current-voltage (I-V) relationships were plotted for +/+ (n=7), EA2/+ (n=3), and EA2/EA2 (n=4) PCs using the voltage protocol shown in (A). Symbols represent mean + SEM. (C) Peak I_{Ba} vs. time was recorded for +/+ and (D) EA2/EA2 PCs during 100 ms depolarizations from −60 to −20

mV. Arrows indicate the sequential addition of Ca^{2+} channel blockers (5 μM nimodipine ($Ca_V1.2$), 3 μM ω-conotoxin MVIIC ($Ca_V2.1$), 1 μM ω-conotoxin GVIA ($Ca_V2.2$)).

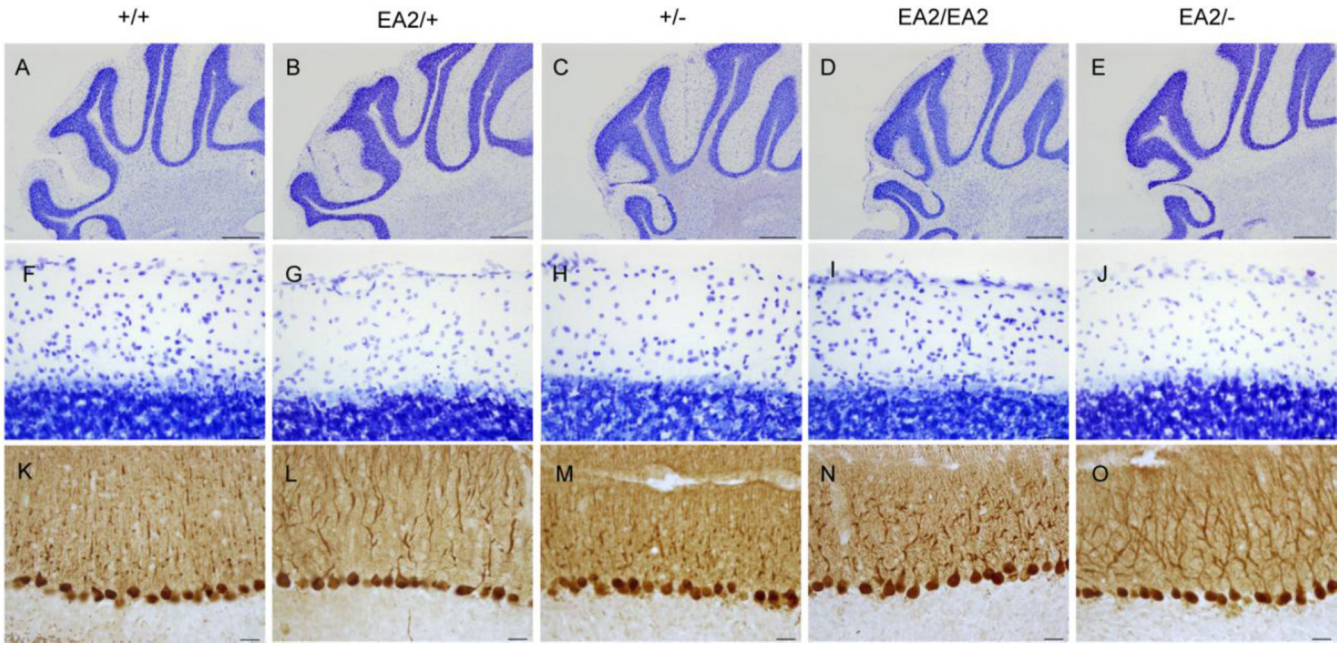

Fig. 3.

Normal cytoarchitecture in the EA2 mutant cerebellum. Examination of cerebella from EA2 mutants stained for Nissl substance (A-J) and calbindin (K-O) revealed no evidence of degeneration (Scale bar A-E=500 μm, F-O=25 μm).

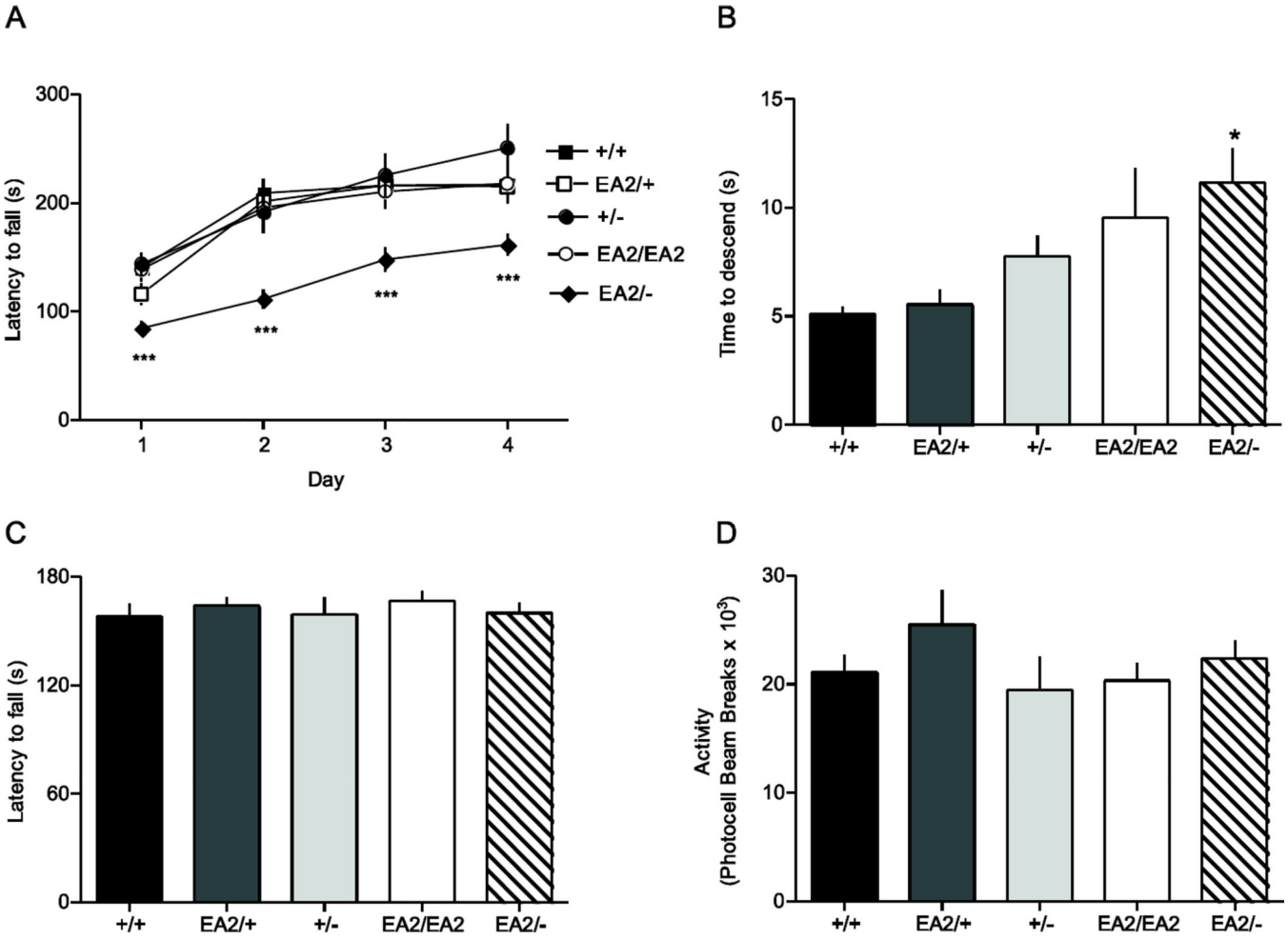

Fig. 4.

Motor phenotype of EA2 mutant mice. Mice carrying various combinations of wild-type (+), knockin (EA2), and knockout (-) *Cacna1a* were tested for their acquisition of motor skills with the accelerating rotarod (A) and pole test (B) as well as grip strength as assessed by the cling test (C) and baseline locomotor activity (D). EA2/- mice (n=17), but not EA2/+ (n=11), +/−(n=10), or EA2/EA2 (n=11) mice showed reduced performance compared to +/+ (n=16) on the rotarod (***p<0.001, Tukey's test) and pole test (*p<0.05, Tukey's test). No significant differences between genotypes were found for cling test ($F_{4,44}$=0.97, P>0.4) or locomotor activity ($F_{4,27}$=0.27, P>0.5).

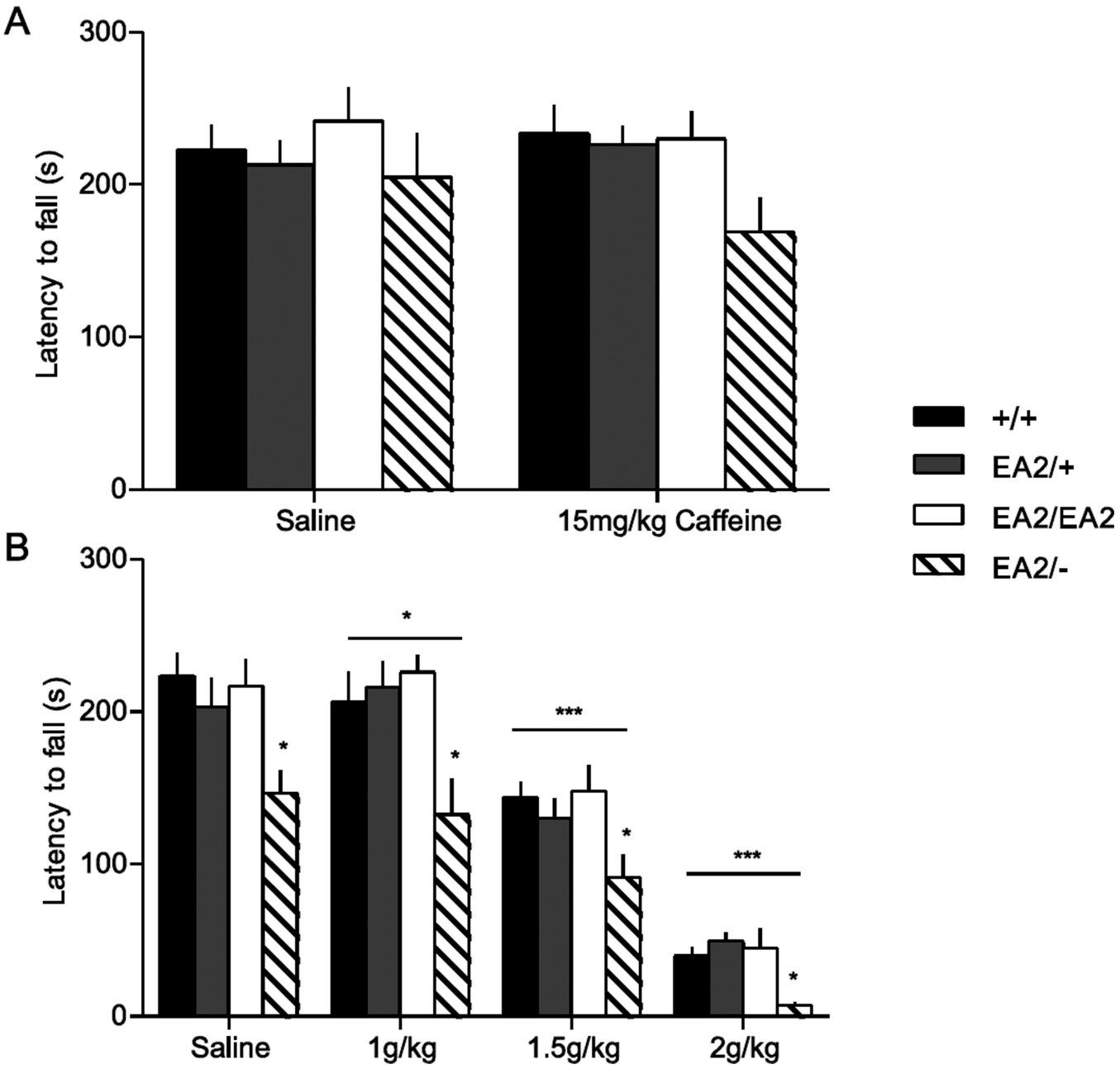

Fig. 5.

Response of EA2 mutant mice to caffeine and EtOH. (A) Rotarod performance was assessed following 15 mg/kg caffeine or saline in +/+ (n=14), EA2/+ (n=11), EA2/EA2 (n=11), and EA2/− (n=6) mice previously trained on rotarod. No main effect of caffeine ($F_{1,38}$=0.24, P>0.5) or interaction between genotype and caffeine ($F_{3,38}$=0.82, P>0.4) were found. (B) Rotarod performance was assessed 20 minutes following EtOH (1,1.5, and 2g/kg) in the same cohort of mice. A significant effect of genotype ($F_{3,38}$=4.73, P<0.01, *p<0.05 for EA2/-) and EtOH dose was found ($F_{3,114}$=167, P<0.001, *p<0.05 for 1g/kg, ***p<0.001 for 1.5g/kg and 2g/kg), but no interaction was found between EtOH and genotype ($F_{9,114}$=0.66, P>0.5).

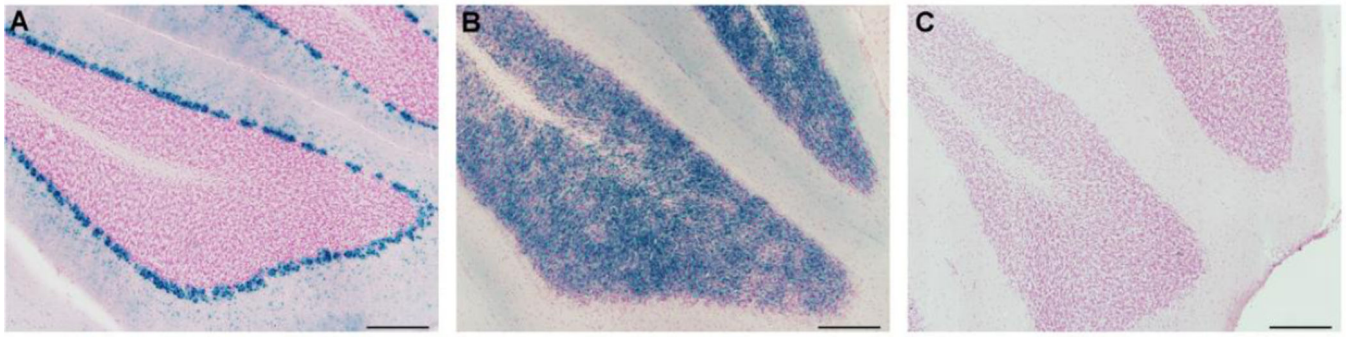

Fig. 6.

X-Gal staining as a reporter for Cre recombinase activity. The Math1-Cre and L7-Cre transgenes were bred onto the Cre reporter line, Rosa26, which expresses β-galactosidase in the presence of Cre recombinase. X-Gal staining, in blue, was located in PCs in L7-Cre expressing mice (A), and in GCs in Math1-Cre expressing mice exposed to tamoxifen at E16.5 (B), but not control mice that did not carry a Cre transgene (C). (Scale bar = 200 μm)

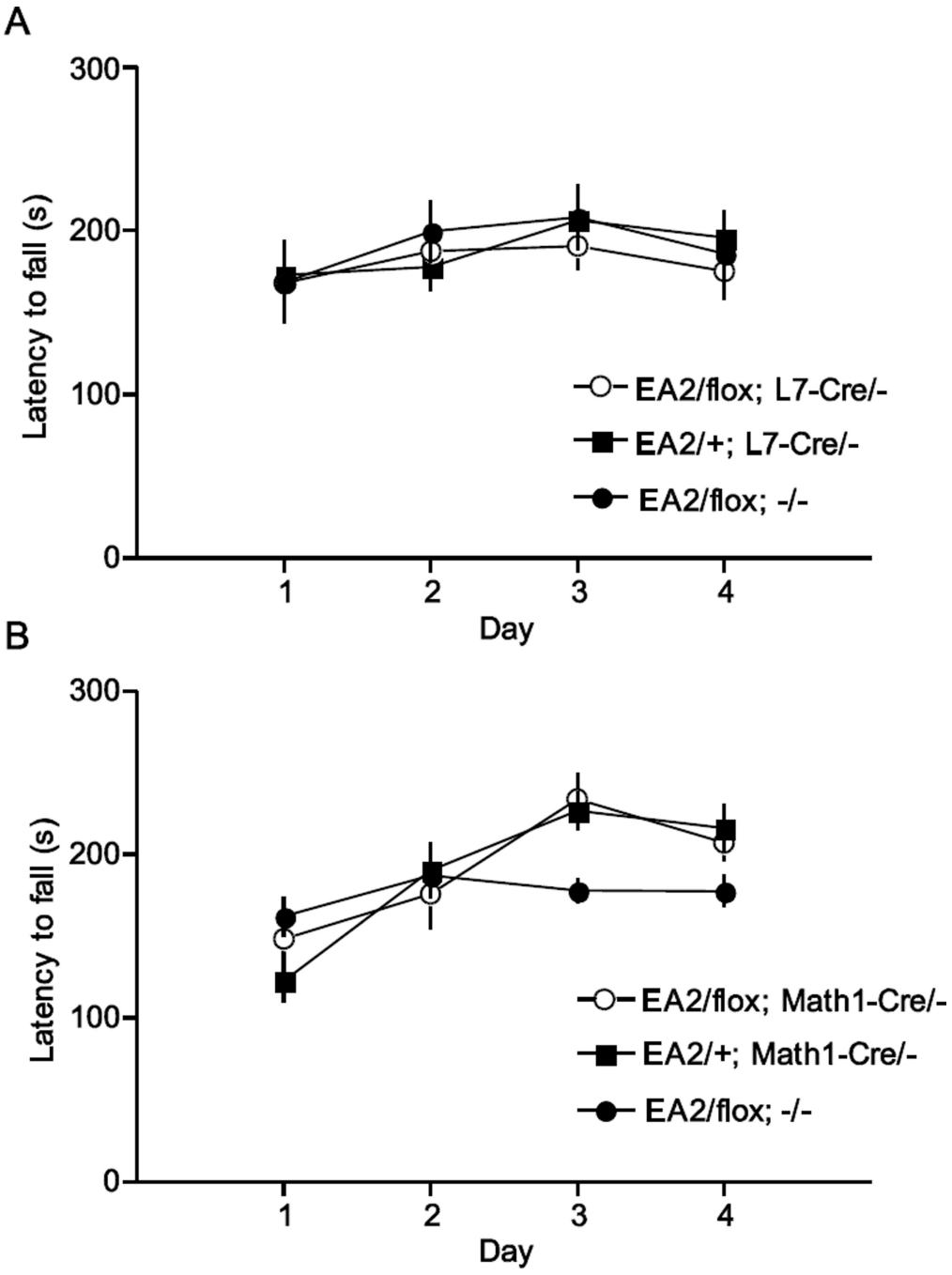

Fig. 7.

Rotarod performance of cell-type specific EA2/- mice. (A) PC-specific EA2/- mice (EA2/flox; L7-Cre/-, n=9) did not exhibit motor dysfunction detectable by rotarod ($F_{2,23}$=0.17, P>0.5) compared to control mice (EA2/+; L7-Cre/-, n=10, EA2/flox, n=7). Similarly, (B) GC-specific EA2/- mice (EA2/flox; Math1-Cre/-, n=10) did not exhibit a motor dysfunction detectable by rotarod ($F_{2,36}$=0.84, P>0.25) compared to control mice (EA2/+; Math1-Cre/-, n=11, EA2/flox, n=14).

Table 1

Nomenclature of mutants used for conditional genetics

Genotype	PCs	GCs	Other cells
EA2/flox; L7-Cre/-	EA2/−	EA2/+	EA2/+
EA2/flox; Math1-Cre/-	EA2/+	EA2/−	EA2/+
EA2/+; L7-Cre/-	EA2/+	EA2/+	EA2/+
EA2/+; Math1-Cre/-	EA2/+	EA2/+	EA2/+
EA2/flox; −/−	EA2/+	EA2/+	EA2/+